Supporting Information

A bimetallic sulfide Co_9S_8/MoS_2/C heterojunction in a three-dimensional carbon structure for increasing sodium ion storage

CHEN Hong, MU Jian-jia, BIAN Yu-hua, GAO Xuan-wen*, WANG Da, LIU Zhao-eng, LUO Wen-bin*

（Institute for Energy Electrochemistry and Urban Mines Metallurgy, School of Metallurgy, Northeastern University, Shenyang 110819, China）

Corresponding author： GAO Xuan-wen, Associate Professor. E-mail: gaoxuanwen@mail.neu.edu.cn;

LUO Wen-Bin, Professor. E-mail: luowenbin@smm.neu.edu.cn

Author introduction： CHEN Hong, Ph.D candidate. E-mail: 2010750@stu.neu.edu.cn

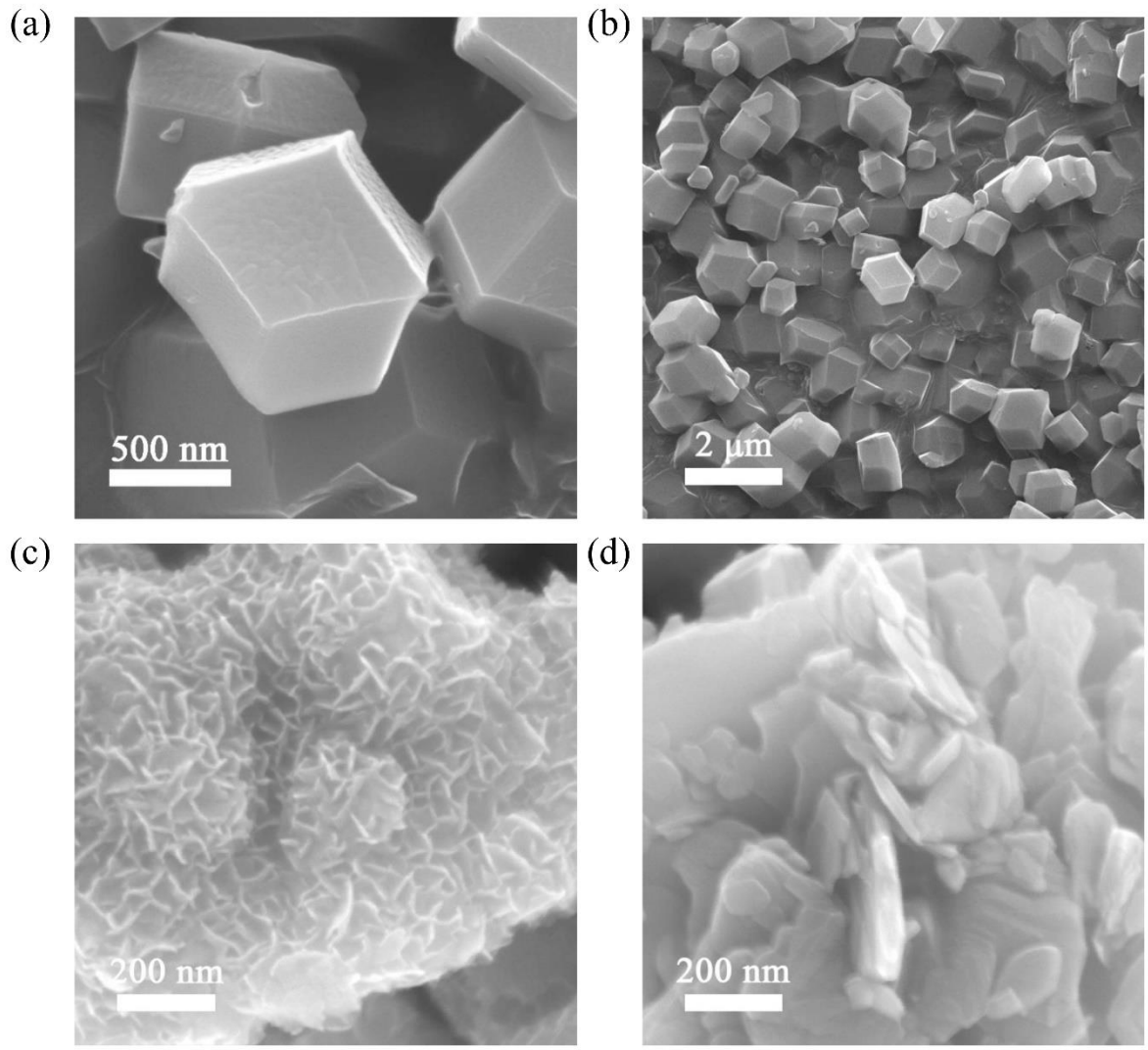

Figure S1 Typical SEM of (a) single ZIF-67 precursor showing the regular shape. (b) Large scale ZIF-67 precursor. (c) Co_9S_8/MoS_2-600, (d) Co_9S_8/MoS_2-800.

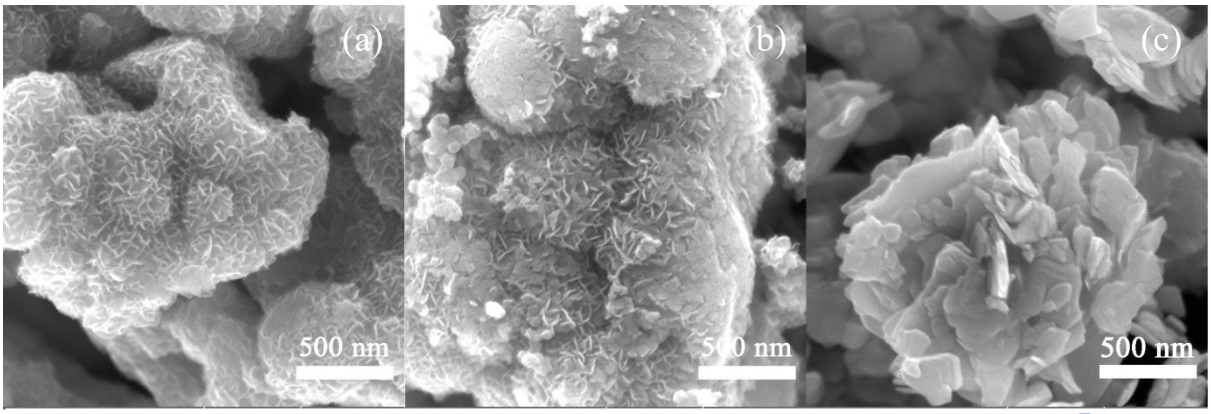

Figure S2 Typical SEM of (a) Co_9S_8/MoS_2-600, (b) Co_9S_8/MoS_2-700 and (c) Co_9S_8/MoS_2-800 heterostructure.

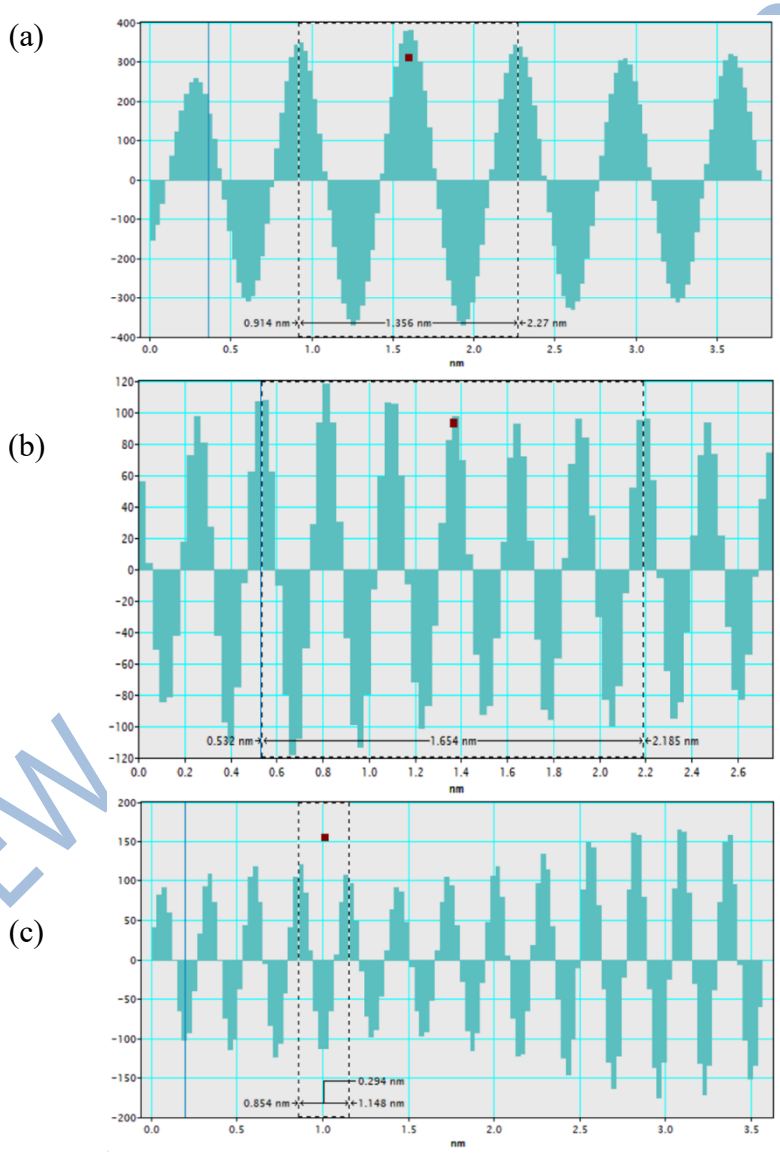

Figure S3 The measured lattice distances of (a) MoS_2 (002), (b) MoS_2 (103) and (c) Co_9S_8 (311) lattice plane.

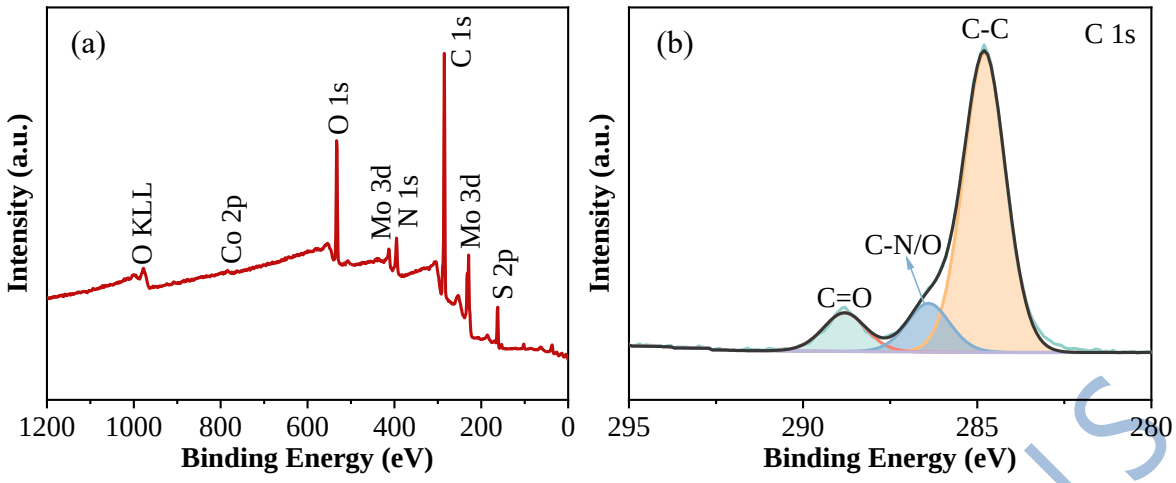

Figure S4 XPS spectra of the Co_9S_8 / MoS_2-700: (a) survey spectra, (b) C 1s spectra.

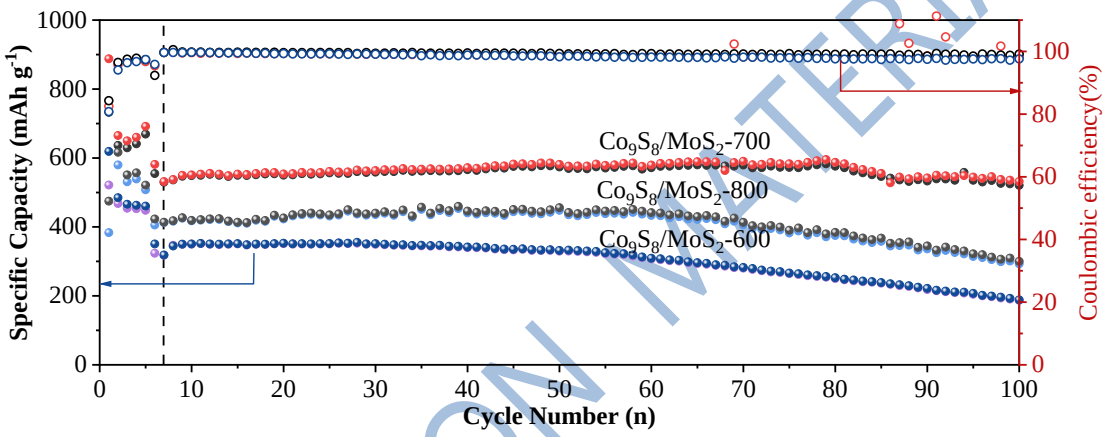

Figure S5 Cycling performance of the Co_9S_8/MoS_2 electrode at 800 mA g^{-1}.

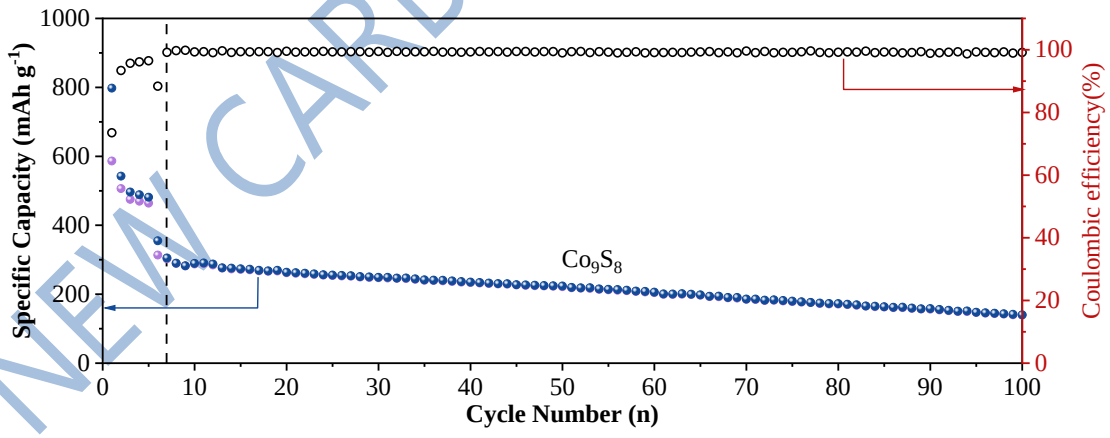

Figure S6 Cycling performance of the Co_9S_8 electrode at 800 mA g^{-1}.

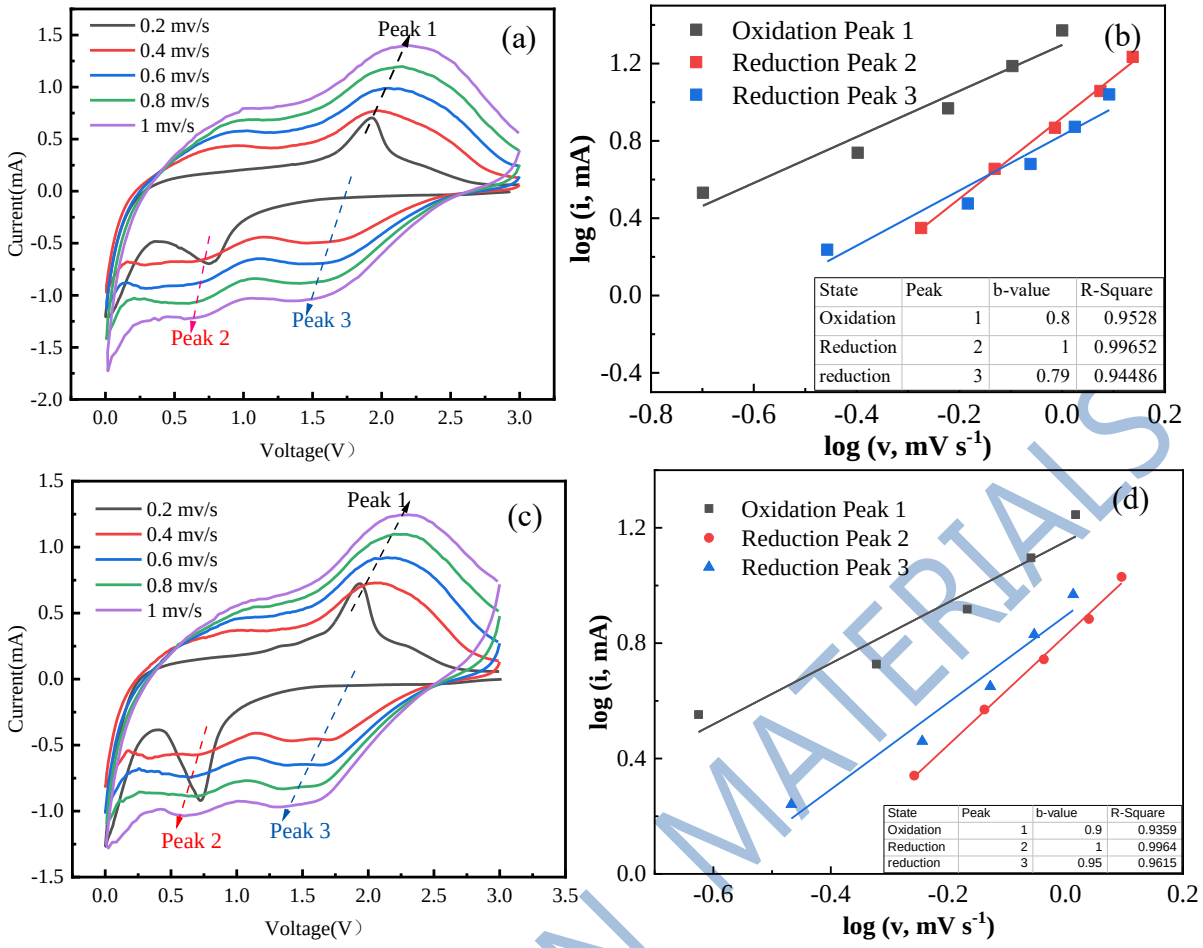

Figure S7 (a, c) CV curves of Co_9S_8/MoS_2-600 and of Co_9S_8/MoS_2-800 at different scan rates, (b, d) log(*i*) versus log(*v*) plots at various redox peaks for Co_9S_8/MoS_2-600 and Co_9S_8/MoS_2-800.

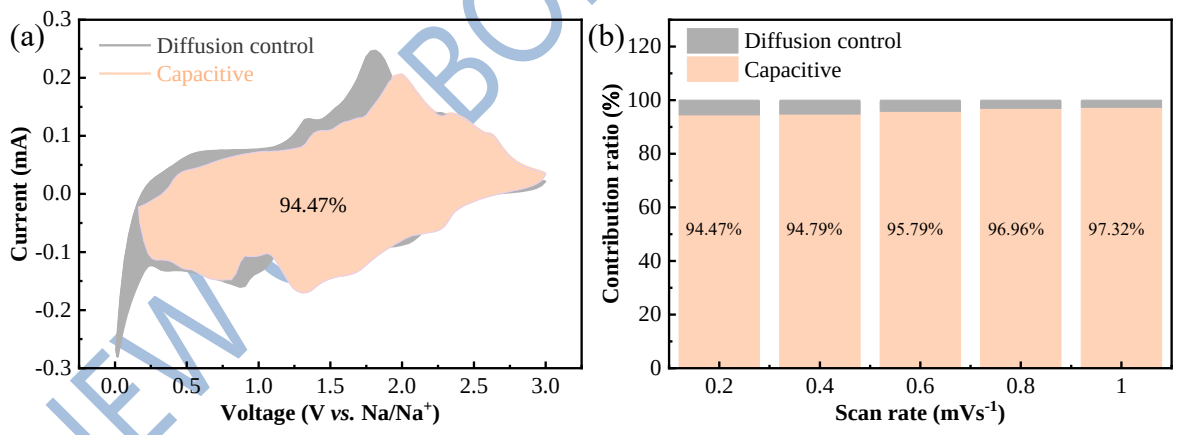

Figure S8 Kinetic analysis of sodium storage behavior of the Co_9S_8/MoS_2-700 electrode: (a). The percentage of capacitive contribution to charge storage at 0.2 mV s^{-1} (b) Capacitive contribution at various scan rates.

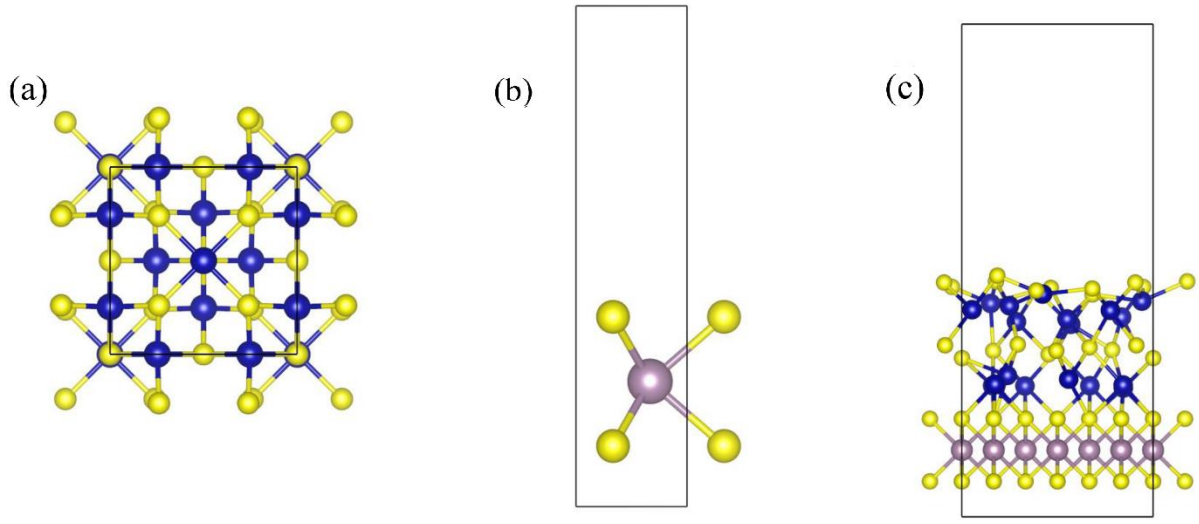

Figure S9 The optimized crystal structures of Co_9S_8, MoS_2 and $Co_9S_8(001)/MoS_2$.

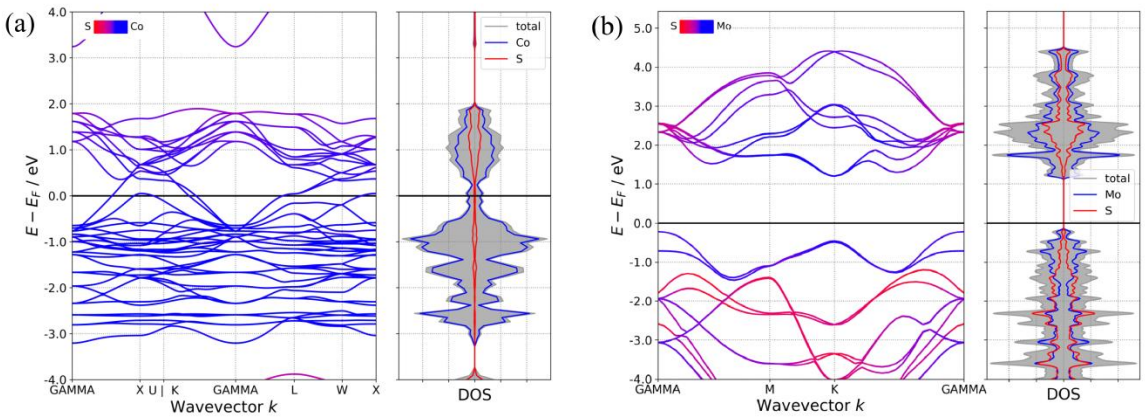

Figure S10 Band structures, calculated for Co_9S_8(a), MoS_2(b). The Fermi level is set to 0.0 eV

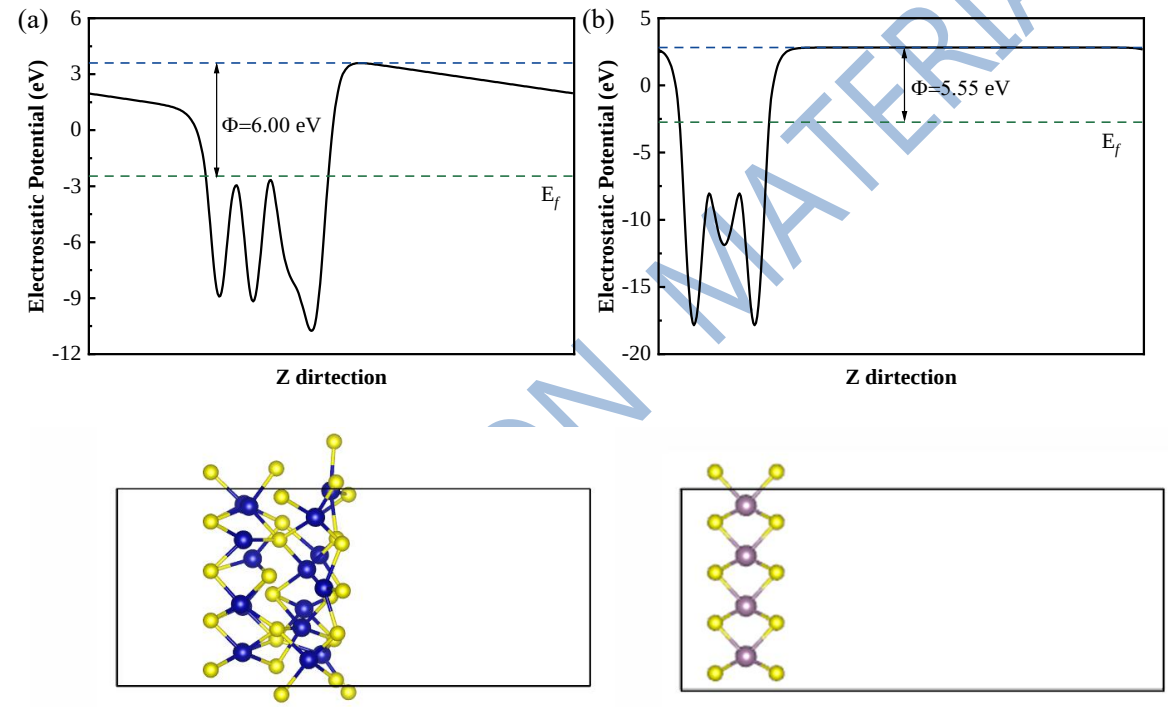

.

Figure S11 Calculated electrostatic potentials for (a) Co_9S_8 (001) surface, and (b) MoS_2 (001) surface. The green and blue dashed lines denote Fermi level and the vacuum energy level, respectively.

Table S1 Comparisons of cycling stability of Co_9S_8/MoS_2 with other Mo-based and Co-based transition metal sulfides.

No.	Samples	Current density (mA g^{-1})	No. of cycles	Capacity (mAh g^{-1})	Refs.
1	MoS_2/RGO Sponge	50	100	372	[1]
2	MoS_2@CNFs	50	50	380	[2]
3	MoS_2@SnO_2@C	100	150	396	[3]
4	Exfoliated MoS_2/G	324	100	100	[4]
5	Graphene@MoS_2@porous graphene	100	100	290	[5]
6	MoS_2 embedded in N-doped carbon fibers	100	100	480	[6]
7	BG-C@MoS_2	100	100	155	[7]
8	MoS_2@SnO_2@C	100	150	396	[8]
9	MoS_2@CNFs	50	50	380	[9]
10	Co_9S_8@carbon yolk-shell	1000	400	426	[10]
11	MoS_2/C	1000	550	340	[11]
12	Co_9S_8@C	500	100	406.5	[12]
13	MWCNTs/Co_9S_8	500	80	444	[13]
14	Co_9S_8-HB	500	100	520	[14]
15	**Co_9S_8/MoS_2-700**	**80**	**100**	**535**	**This work**
		2000	**120**	**464**	

References

[1] Li J L, Qin W, Xie J P, et al., Rational Design of MoS_2-Reduced Graphene Oxide Sponges as Free-Standing Anodes for Sodium-Ion Batteries[J].Chemical Engineering Journal, 2018, 332: 260-266.

[2] Wang G M, Bi X X, Yue H L, et al., Sacrificial Template Synthesis of Hollow C@MoS_2@PPY Nanocomposites as Anodes for Enhanced Sodium Storage Performance[J]. Nano Energy, 2019, 60: 362-370.

[3] Chen Z, Yin D G, and Zhang M, Sandwich-Like MoS_2@SnO_2@C with High Capacity and Stability for Sodium/Potassium Ion Batteries[J]. Small, 2018, 14(17).

[4] Wang B, Xia Y, Wang G, et al., Core Shell MoS_2/C Nanospheres Embedded in Foam-Like Carbon Sheets Composite with an Interconnected Macroporous Structure as Stable and High-Capacity Anodes for Sodium Ion Batteries[J]. Chemical Engineering Journal, 2017, 309: 417-425.

[5] Hao X, Jiang Z, Shang X, et al., Understanding the Role of Graphene Intercalation Layers on Both Sides of Sandwich Structured Graphene@MoS_2@Porous Graphene Anode in Promoting Sodium Storage Performance and Stability[J]. Journal of Alloys and Compounds, 2020, 845: 155336.

[6] Cheng A, Zhang H, Zhong W, et al., Few-Layer MoS_2 Embedded in N-Doped Carbon Fibers with Interconnected Macropores for Ultrafast Sodium Storage[J]. Carbon, 2020, 168: 691-700.

[7] Zhou H, Lv P, Lu X, et al., Fibrous Network of C@MoS_2 Nanocapsule-Decorated Cotton Linters Interconnected by Bacterial Cellulose for Lithium- and Sodium-Ion Batteries[J]. ChemSusChem, 2019, 12(23): 5075-5080.

[8] Chen Z, Yin D, and Zhang M, Sandwich-Like MoS_2@SnO_2@C with High Capacity and Stability for Sodium/Potassium Ion Batteries[J]. Small, 2018, 14(17): 1703818.

[9] Chen C, Li G Q, Lu Y, et al., Chemical Vapor Deposited MoS_2/Electrospun Carbon Nanofiber Composite as Anode Material for High-Performance Sodium-Ion Batteries[J]. Electrochimica Acta, 2016, 222: 1751-1760.

[10] Zhao Y Y, Fu Q, Wang D S, et al., Co_9S_8@Carbon Yolk-Shell Nanocages as a High Performance Direct Conversion Anode Material for Sodium Ion Batteries[J]. Energy Storage Materials, 2019, 18: 51-58.

[11] Tang Y C, Zhao Z B, Wang Y W, et al., Ultrasmall MoS_2 Nanosheets Mosaiced into Nitrogen-Doped Hierarchical Porous Carbon Matrix for Enhanced Sodium Storage Performance[J]. Electrochimica Acta, 2017, 225: 369-377.

[12] Zhang Y H, Wang N N, Xue P, et al., Co_9S_8@Carbon Nanospheres as High-Performance Anodes for Sodium Ion Battery[J]. Chemical Engineering Journal, 2018, 343: 512-519.

[13] Zhou H P and Hu J, Facile Synthesis of Multi-Walled Carbon Nanotubes/Co_9S_8 Composites with Enhanced Performances for Sodium-Ion Battery[J]. Materials Letters, 2017, 195: 26-30.

[14] Yin M M, Zhao D, Feng C H, et al., Construction of Porous Co_9S_8 Hollow Boxes with Double Open Ends toward High-Performance Half/Full Sodium-Ion Batteries[J]. Acs Sustainable Chemistry & Engineering, 2020, 8(16): 6305-6314.